Journal of Chromatography A, 1218 (2011) 4434–4444

Contents lists available at ScienceDirect

Journal of Chromatography A

journal homepage: www.elsevier.com/locate/chroma

# Analytical methodology for multidimensional size/branch-length distributions for branched glucose polymers using off-line 2-dimensional size-exclusion chromatography and enzymatic treatment

Francisco Vilaplana, Robert G. Gilbert*

*Centre for Nutrition and Food Sciences (CNAFS), University of Queensland, Hartley Teakle Building, Brisbane, Queensland 4072, Australia*

ARTICLE INFO

*Article history:*
Received 4 January 2011
Received in revised form 13 March 2011
Accepted 9 May 2011
Available online 14 May 2011

*Keywords:*
Size-exclusion chromatography (SEC)
Branched polysaccharides
Size distributions
Branching structure
Starch
Glycogen

ABSTRACT

Instrumental and procedural optimizations are developed for a new method to obtain 2-dimensional distributions for branched homopolymers based on size and branching. The method uses 2-dimensional off-line size-exclusion chromatography (SEC) and chemical debranching, in this case using debranching enzymes on branched glucose polymers. This treatment, first presented for the 2D weight and number distributions of starch [F. Vilaplana, R.G. Gilbert, Macromolecules 43 (2010) 7321] is applied here to give 2D weight distributions as functions of size and branch length for glycogen, amylose, and native starch containing both amylopectin and amylose. Completely dissolved polysaccharides are first fractionated by size (hydrodynamic volume) using preparative SEC; the collected fractions are then debranched by addition of isoamylase, and the size distributions of the corresponding branches are analyzed for each fraction using analytical SEC with differential refractive index and with multiple-angle laser light scattering detection. Operational parameters have been optimized to provide sufficient separation resolution for each dimension (size of the whole branched macromolecule and size of the resulting branches after debranching) and to minimize degradation. These 2-dimensional distributions bring out new features in the structure of these branched polysaccharides, and offer a useful tool to elucidate relations between biosynthesis, structure, and properties.



## 1. Introduction

Glycogen and starch are hyperbranched polymers (also referred as branch-on-branch polymers; there is as yet no IUPAC definition of 'hyperbranched') of glucose, comprising α-D-glucopyranosyl (anhydroglucose) monomeric units linearly extended by α-(1→4) linkages and with branches formed by α-(1→6) bonds. Obtaining detailed knowledge about the biosynthesis/(bio)degradation–structure–property relations of these molecules is the key for understanding their functionality in biological systems and to tailor their properties and applicability through (bio)synthetic and physicochemical modification, with implications for nutrition and health, biotechnology, and material sciences. Glycogen molecules have an average branch chain length of 10–14 glucose units, with a branching degree of 7–9%, and average molecular weights between $10^5$ and $10^8$ g mol$^{-1}$ [1–3]. Starch comprises two main macromolecular populations with distinct branching architecture: amylose and amylopectin [4]. Amylose is a relatively small glucose polymer containing few long-chain branches and molecular weights up to $10^5$–$10^6$ g mol$^{-1}$. Amylopectin is a large hyperbranched macromolecule with a similar branching structure to glycogen containing large numbers of short-chain branches and molar masses ranging between $10^7$ and $10^9$ g mol$^{-1}$. The chain-length distribution of the individual branches from glycogen and starch has been well characterized; the characterization of the whole macromolecular structure still constitutes a challenge.

Size-separation techniques such as size-exclusion chromatography (SEC) and field-flow fractionation (FFF) provide experimental 1D distributions based on their separation parameter, the hydrodynamic volume $V_h$. The definition of $V_h$ depends on the technique [5], and for SEC, this separation parameter is usually considered to be proportional to the product of the weight-average intrinsic viscosity with the number-average molar mass [6–8], although no universal agreement has been reached on this point. These distributions include the number distribution, $N(V_h)$, the weight distribution, $w(\log V_h)$, the size dependence of weight-average molecular weight, $\overline{M}_w(V_h)$, and the size dependence of the number-average molecular weight, $\overline{M}_n(V_h)$ [9,10]. Emerging separation

* Corresponding author. Tel.: +61 7 3365 4809; fax: +61 7 3365 1188.
*E-mail address:* b.gilbert@uq.edu.au (R.G. Gilbert).

0021-9673/$ – see front matter © 2011 Elsevier B.V. All rights reserved.
doi:10.1016/j.chroma.2011.05.027

procedures such as molecular-topology fractionation (MTF) [11,12] or temperature-gradient interaction chromatography (TGIC) [13] have been reported to separate synthetic macromolecules by their branching architecture; however, their topological separation mechanism is not fully understood and they have not yet been implemented for branched polysaccharides. Coupling of two-dimensional chromatographic modes combining interaction, topological, or size separations could potentially provide multidimensional structural distributions [14–17], but their application to branched glucose polysaccharides still constitutes a technical challenge.

In this work, a different approach is followed to obtain 2D structural distributions for branched polysaccharides based on macromolecular size and branch chain-length, combining multidimensional offline SEC and enzymatic debranching. The first implementation of this has been reported earlier for starch [18], itself building on pioneering work by Ball and co-workers [19] and Jane and co-workers [20]. The present paper systematically develops and optimizes the original methodology [18] and explores the separation science needed to optimize this procedure, as well as giving the first application of these improved methods to amylose and glycogen. The procedure uses the fact that starch and glycogen can be debranched with debranching enzymes to cleave the branching α-(1 → 6) bonds quantitatively; quantitative debranching is also possible (using appropriate reagents) with a very restricted range of branched synthetic polymers (e.g. [21]). Various requirements, such as complete dissolution, minimization of degradation during sample preparation and separation, sufficient sample collection during size fractionation, complete debranching, and optimized separation resolution for both macromolecular size of the fully branched molecules and the size of the branches must be met to provide meaningful 2D distributions.

The theory behind these 2D distributions was first sketched in previous work [10,18] but here some definitions are corrected and the technique extended. The object is to obtain the 2D number distribution in terms of total molecular size and degree of polymerization of a branch. The number distribution $N(V_h, X_{de})$ is defined as the number of branches of DP $X_{de}$ in an sample of parent (fully branched) polymers of hydrodynamic volume $V_h$, which is equivalent to the corresponding weight distribution $w(\log V_h, \log X_{de})$ through Eq. (1) (see Supplementary Material for the full mathematical treatment).

$$w(\log\ V_h, \log X_{de}) = X_{de}^2\, N(\log V_h, X_{de}) \quad (1)$$

These distributions could be theoretically obtained by a comprehensive 2-dimensional SEC × SEC chromatographic system satisfying the following ideal conditions: if (1) there were no band broadening during each size separation step (both the macromolecular size – first dimension – and the chain-length of the branches, second dimension), (2) in the first SEC step, one were able to take elution slices that had an infinitesimal range of $V_h$, (3) then perform enzymatic debranching instantaneously and in-line on each elution slice, and finally (4) analyze the resulting branches in the second separation dimension to obtain the debranched size (debranched hydrodynamic volume $V_{h,de}$), or equivalently debranched DP $X_{de}$, of the branches for each elution slice with $V_h$. In that case, each of these infinitesimal elution slices $dV_{el}$ from the first size separation dimension would contain an infinitesimal hydrodynamic volume increment $dV_h$. Each ideal elution slice would contain a range of molecular weights, because SEC separates by size, not molecular weight, and branched polymers with different molecular weights and branching structures can have the same hydrodynamic volume. Hence each $dV_h$ fraction would have internal dispersity $\overline{M}_w/\overline{M}_n = D > 1$ ('dispersity' is the IUPAC term [22] to replace what has hitherto been termed 'polydispersity', 'polydispersity index', etc.). The ideal analytical SEC step on the fully branched samples would show infinitely narrow signals from all detectors, because the separation in hydrodynamic volume would have been ideal: that is, $N(V_h)$, $w(\log V_h)$ and $\overline{M}_w(V_h)$ would all be delta functions. If (in this ideal case) one were to use a mass-sensitive detector on the subsequent debranched distributions, one would then obtain the desired 2D distribution $w(\log V_h, \log V_{h,de})$ (or equivalent distribution).

In practice, this ideal situation is unachievable because of a series of technical issues: (i) band-broadening is relatively poor in the first SEC step, which is preparative SEC so as to obtain sufficient quantities for subsequent debranching, and hence the elution slices contain a significant range of hydrodynamic volumes, (ii) the debranching process needs to be performed offline with small but significant volume of the analyte (see Section 2.5), (iii) the second-dimension analysis of the chain-length distribution of the resulting branches is not a fast separation and cannot be performed on-line with the preparative step, (iv) band broadening means that both the first and second separation steps contain a range of $V_h$. Instead of the ideal case, approximate 2D distributions are obtained by an off-line procedure combining preparative and analytical SEC and enzymatic debranching as follows [18], and as shown in Fig. 1, which compares the ideal 2D online chromatographic methodology with the offline procedure used here. The (suitably normalized) signal from the mass-sensitive detector is still treated as yielding $w(\log V_h, \log V_{h,de})$. However, the dependent variables are obtained as follows. $V_h$, or equivalently the hydrodynamic radius $R_h$ (not to be confused with the Stokes radius; here $R_h$ is directly derived from $V_h = 4/3\ \pi\ {R_h}^3$ and is often referred to as the viscometric radius $R_\eta$), is taken to be the average size of (fully branched) polymers in that elution slice $(\overline{R}_h)_{br}$, this average being defined by Eq. (2) below. The value of $X_{de}$, or equivalently the corresponding (debranched) hydrodynamic radius $(R_h)_{de}$, is taken to be the average $\overline{X}_{de}$ obtained either by MALLS measurements of the $\overline{M}_w$ of the SEC elution of the debranched sample, or $(R_h)_{de}$ obtained by universal calibration. The normalization is such that the area under each debranched SEC weight distribution for each elution volume slice is proportional to the relative amount of starch in that slice.

The chain-length distribution of oligosaccharides up to degree of polymerization DP ∼ 85 is best obtained using fluorophore-assisted capillary electrophoresis (FACE) [23,24]. However, this technique fails to give information about the chain-length distributions of longer linear polysaccharides in the range of amylose branches. Instead, SEC is used here as the second analytical dimension for obtaining the size distributions of the branches of the target polysaccharides (glycogen, amylose and native starch), taking into account that individual DP resolution cannot be achieved due to lack of sufficient separation resolution. Future extensions of the present method could use FACE for lower DPs and SEC for the higher ones, with band-broadening corrections for the SEC data.

## 2. Experimental

### 2.1. Materials

Commercial oyster glycogen (Sigma Aldrich, Sigma–Aldrich, St. Louis, MI, USA) and commercial amylose (Sigma–Aldrich, St. Louis, MI, USA) were used as provided. Native starch from Malaysian rice flour (MRQ74) from MARDI (Kuala Lumpur, Malaysia) was extracted from the whole rice grain using methylsulfinylmethane (dimethyl sulfoxide, DMSO; ACS grade, Merck, Australia) prior to method development. The rice flour has a starch content of 84.28 ± 0.23% as found using the Total Starch Kit (Megazyme, Wicklow, Ireland) and an amylose content in starch of 27% as reported by the supplier.

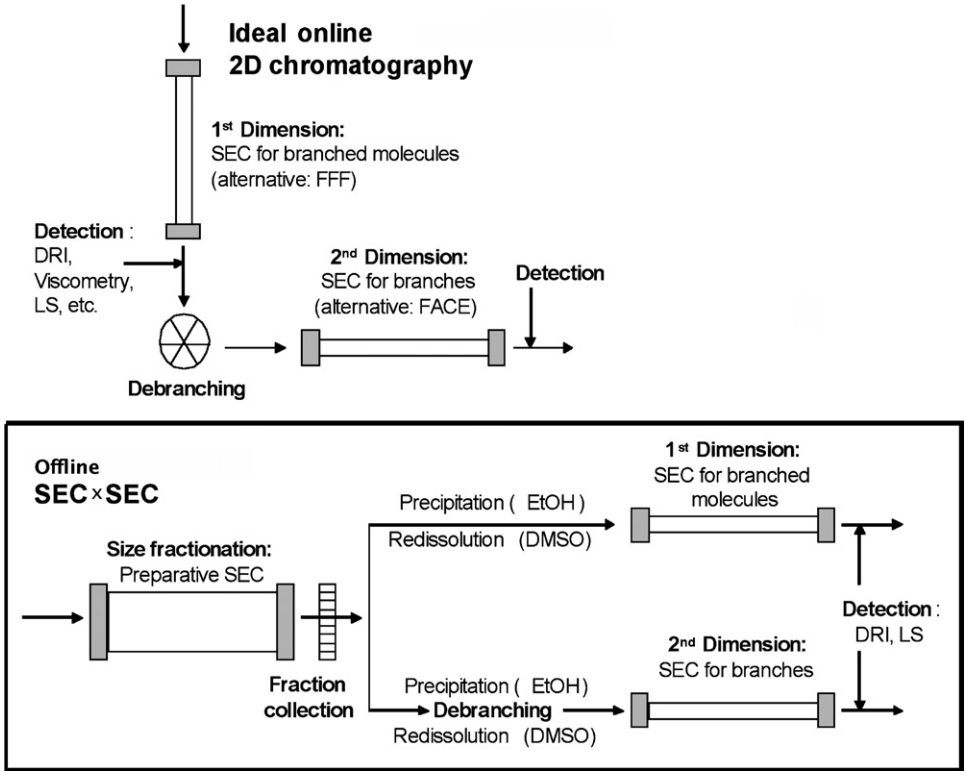


**Fig. 1.** Schematic comparison between an ideal online 2-dimensional SEC × SEC set-up and the offline methodology used here, which combines preparative and analytical SEC with enzymatic debranching to obtain the 2-dimensional size/branch distributions for branched polysaccharides.

### 2.2. Dissolution of the polysaccharide samples

SEC eluent consisting of filtered DMSO with 0.5% (w/w) LiBr (ReagentPlus) was employed for sample dissolution and size separation. Glycogen, amylose and rice starch with concentrations ranging from 2 to 50 g $L^{-1}$ were dissolved directly in the SEC eluent in a thermo-mixer set at 80 °C for 8 h without stirring.

### 2.3. Fractionation by size using preparative SEC

Polysaccharide samples were fractionated using a AF2000 preparative SEC set-up (Post-Nova Analytics, Landsberg-Lech, Germany), consisting of an isocratic pump, an online degasser, a column oven, and a refractive index detector. The fractionation was achieved using a combined preparative column set including a PREP GRAM pre-column, a PREP GRAM 30 and PREP GRAM 3000 columns made of a polyester copolymer network from Polymer Standards Services (PSS, Mainz, Germany) kept at 80 °C and with DMSO/LiBr 0.5% (w/w) as mobile phase. Various operational parameters were optimized, including injected sample amount (sample concentration and injection volume) and flow rate. Manual injections of 1 and 2 mL samples were performed using a Rheodyne 7000 high-pressure switching valve (IDEX Health & Science LLC, Rohnert Park, CA, USA). Different flow rates, between 0.5 and 3 mL $min^{-1}$, were tested to assess the effects of shear scission during the fractionation process. Fractions were collected manually at different elution volumes (and hence fractionated by hydrodynamic volume) after they reached the refractive index detector. An aliquot of each fraction was taken for further analysis using the analytical SEC set-up for branched molecules; the aliquots were precipitated, centrifuged, and redissolved in DMSO/LiBr before injection into the SEC. The remaining sample from each fraction was precipitated, centrifuged, and subjected to the debranching procedure prior to final SEC analysis using the set-up for debranched molecules.

### 2.4. Precipitation and centrifugation

The collected fractions from preparative SEC in DMSO/LiBr were precipitated using absolute ethanol (Analysis Grade, Merck, Australia) in proportions 5:1 (v/v) (ethanol:DMSO) and leaving the solutions overnight. The precipitated solutions were centrifuged at 1392 × *g* in an Allegra X-12 R centrifuge (Beckman Coulter, Brea, CA, USA) and the supernatant was discarded. Complete precipitation of the starch fraction was verified independently using (i) the Total Starch Kit (Megazyme, Wicklow, Ireland) and (ii) by comparison of the size SEC distributions before and after precipitation.

### 2.5. Debranching of polysaccharide fractions

The precipitated fractions were debranched with isoamylase from *Pseudomonas* sp. (Megazyme, Wicklow, Ireland) with specific activity 280 U/mg (40 °C, pH 3.5, oyster glycogen) using the following standard procedure. The starch fractions were dispersed with 9 mL deionized water, heated in a boiling water bath for 15 min and then cooled to room temperature. 20 μL of sodium azide solution in deionized water (0.1 g $mL^{-1}$), 1 mL of 0.1 M sodium acetate buffer (pH 3.5), and 5 μL of the enzyme solution were transferred. The mixture was vortexed, incubated in a water bath at 37 °C for 4 h, placed in boiling water for 15 min to deactivate the enzyme, and immediately placed in a freezer to avoid retrogradation of the debranched chains. That this procedure does not cause retrogradation was shown in our group by Dr. Jovin Hasjim, who compared the amount of dissolved starch in DMSO with fresh samples and samples after freeze-drying; the observation that the total amount of dissolved starch was the same with experimental uncertainty is taken as proof of absence of retrogradation, because retrograded starch does not dissolve easily in DMSO. Finally, the samples were freeze-dried in a VirTis Benchtop K freeze-dryer (VirTis, Gardiner, NY, USA).

### 2.6. Offline analytical SEC of branched and debranched fractions

Analytical SEC analyses of the branched and debranched fractions were performed using an Agilent 1100 series set-up, with an isocratic pump, an autosampler injecting from a 1000 μL piston without temperature control, an online degasser, and an Agilent 1100 series column oven at 80 °C. Detection was carried out using a multiple-angle laser light scattering (MALLS; BIC-MwA7000, Brookhaven Instrument Corp., New York), and a RID-10A refractive index detector (Shimadzu, Kyoto, Japan) both operating at 635 nm and thermostated at 45 °C. Separation of the 'branched' fractions was carried out using combined GRAM PreColumn, 30 and 3000 analytical columns (PSS) at 0.3 mL $min^{-1}$, whereas analyses of the debranched fractions was performed with combined GRAM PreColumn, 10 and 1000 analytical columns (PSS) at 0.6 mL $min^{-1}$. The chromatographic conditions and the different column set-ups have been optimized for separation of branched and debranched starch samples, respectively, minimizing the effects of shear scission of the amylopectin in the case of the branched set-up, and, in the case of the debranched set-up, allowing full separation of the debranched chain lengths from the amylose and amylopectin components of starch [25,26].

### 2.7. SEC calibration and data processing

Mark–Houwink (universal) calibrations of the preparative and the analytical SEC set-ups were performed by injection of pullulan standards with molecular weights ranging from 342 to $1.66 \times 10^6$ g $mol^{-1}$, provided by PSS. The Mark–Houwink parameters for pullulan in DMSO/LiBr (0.5 wt%) at 80 °C are $K = 2.427 \times 10^{-4}$ dL $g^{-1}$ and $a = 0.6804$ (Kramer and Kilz, PSS, private communication). The calibration procedure and the resulting curves for the different SEC set-ups are presented as Supplementary Data. The data recorded after the analytical SEC separations and multiple detection was processed using WinGPC software (PSS) and further analyzed by additional procedures to obtain the SEC weight distribution, $w(\log V_h)$, and the size dependence of the weight-average molecular weight, $\overline{M}_w(V_h)$ [10,18] (see Supplementary Data).

## 3. Results and discussion

### 3.1. Optimization of the size fractionation of branched polysaccharides using preparative SEC

Preparative SEC was applied to the branched polysaccharide samples to collect different fractions with sufficient separation resolution based on hydrodynamic volume and with enough sample content to perform subsequent enzymatic debranching and size-separation analysis of the branched and debranched fractions.

DMSO with low additions of lithium salts such as LiBr has been shown to completely dissolve starch minimizing degradation during sample preparation, and it also can assist to remove some of lipids and proteins [27,28]. Complete dissolution of native starch in DMSO/LiBr (0.5%, w/w) was verified using the Total Starch Kit (Megazyme, Wicklow, Ireland), with dissolution percentages up to 100 ± 5%. Complete recovery after SEC separation was verified using the Total Starch Kit on the collected eluted sample after separation, and by calculation of the eluted mass using the DRI detector and the correspondent d$n$/d$c$ values.

Different operational parameters were optimized for preparative SEC in order to achieve a good compromise between sufficient injected sample for effective fraction collection, separation resolution, and minimizing artifacts due to shear scission or anomalous elution behaviour. A suitable sample amount per collected fraction was estimated to be 2 mg, taking into account suitable injection concentrations and volumes for analytical SEC separations (1–2 g $L^{-1}$ and 100 μL, respectively) and the necessary sample weight to perform quantitative enzymatic debranching. An average of 8–10 fractions per sample were estimated as offering reliable multidimensional distributions based on macromolecular size and subsequent debranching, taking into account the experimental limitations of fractionation by preparative SEC and enzymatic debranching. The amount of injected sample was controlled by varying the sample concentration and the injected volume; different combinations were tested to achieve optimal sample fractionation with suitable separation resolution without column overloading. A range of mobile phase flow rates was also investigated to minimize the shear scission of the large branched polysaccharides and to optimize the separation resolution during preparative SEC.

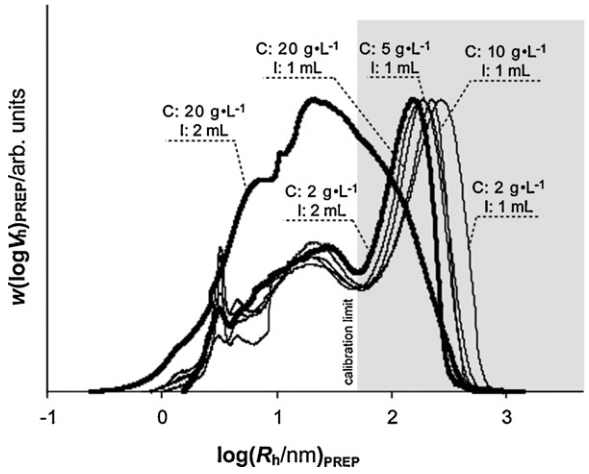


**Fig. 2.** Effect of injected rice starch sample on the $w(\log V_h)$ size distribution profile from preparative SEC: I (injection volume); C (injected concentration). The grey area corresponds to the extrapolated calibration region. Distributions normalized to the area under the curve.

Sample concentration during injection should be maintained in the diluted regime to achieve improved separation resolution and avoid overloading. The critical overlap concentration ($c^*$), the transition concentration between the diluted and the semi-diluted regime, was measured for native starch in DMSO/LiBr using complex viscosity measurements in a rheometer (see Supplementary Data). The transition from dilute to semi-diluted regimes was observed to occur between 20 and 30 g $L^{-1}$ for native starch, in agreement with similar studies [29], so this concentration was used as the upper limit for sample dissolution. Glycogen and amylose are expected to have higher $c^*$ than starch due to the lower molecular weight (in the case of amylose) and denser branching structure (for glycogen), so the assumption of the upper concentration limit for native starch is safe for those polysaccharides.

Different combinations of injection volumes (1 and 2 mL) and concentrations (2–20 g $L^{-1}$) were tested for rice starch to analyze the effect of injected sample weight (2–40 mg) on the separation resolution and to optimize the sample amount that could be fractionated with preparative SEC. Fig. 2 shows the SEC $w(\log V_h)$ distributions for different injected sample weight conditions (different values of the product of the injected volume and injected sample concentration, $V_{inj} \times c_{inj}$) of rice starch. A typical bimodal sized distribution for starch is observed, with the amylopectin peak (at $R_h \sim 300$ nm, or $\log R_h/\text{nm} \sim 2.5$) and amylose peak (at $\log R_h/\text{nm} \sim 1.5$). Some lipid and protein contaminations can be observed at lower sizes ($\log R_h/\text{nm} \sim 0.5$). Higher injected sample weight results in a shift of the amylopectin peak towards lower $R_h$ values; this is a well-known local pore column overloading

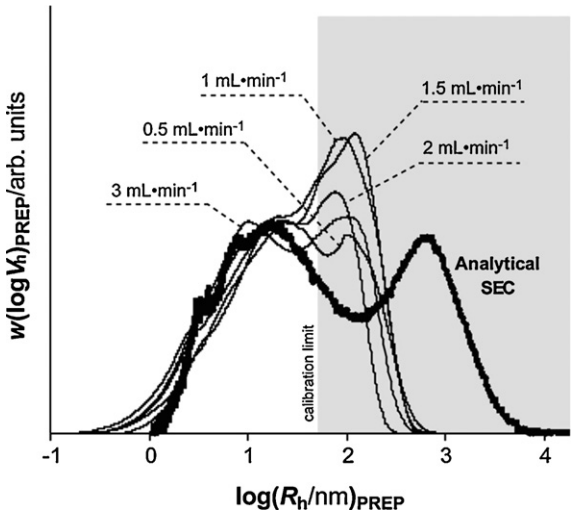


**Fig. 3.** Effect of mobile phase flow rate on the $w(\log V_h)$ size distribution for rice starch in preparative SEC (thin lines) compared to analytical SEC (thick line). The grey area corresponds to the extrapolated calibration region. Distributions normalized to the peak of the amylose component.

effect in SEC that causes elution of larger macromolecules to higher retention volumes and subsequent loss of resolution [30]. Column overloading is especially evident when a total injected mass of 40 mg (2 mL of 20 g $L^{-1}$) of rice starch was injected, with a quite distorted size distribution. Theoretically, the minimal amount of sample giving an adequate signal-to-noise ratio should be injected; however, for fractionation purposes where high amounts of solute need to be collected, a compromise is required between injected sample and resolution. In our case, an injection mass of 20 mg (1 mL × 20 g $L^{-1}$) was selected to perform the size fractionations for the polysaccharides.

The effect of flow rate during preparative SEC was studied for rice starch by testing different values between 0.5 and 3 mL $min^{-1}$. Flow rate has a significant influence on the separation resolution and also on shear scission. Shear scission of high-molecular-weight macromolecules has been proven to occur during size separations in porous columns. Degradation is expected to occur not only in the pore boundaries and interparticular channels, but in the extra-column plumbing as well [31,32]. In the case of starch separations, shear scission of the amylopectin component is a matter of special interest. A recent study [25] based on similar experimental data, and developing a quantitative analogy to droplet shear, suggested that there are no physical conditions during SEC separations that could fully avoid shear scission of the amylopectin component without major advances in the technology. This limitation of SEC must be considered during our fractionation experiments (see Supplementary Data). Fig. 3 shows the size distributions of native rice starch from preparative SEC for different flow rates, compared with the size distribution obtained for the same starch sample using analytical SEC. The size distributions from preparative SEC show very different profiles in the amylopectin region compared with those from analytical SEC, because much of the amylopectin size range was in the pore exclusion limit of the SEC columns (both preparative and analytical) employed here, and also due to extrapolation uncertainties of the calibration curve (see Supplementary Data). However, the distributions obtained from preparative SEC using different flow rates show very similar profiles in the amylose region when compared with the distributions obtained from analytical SEC. Only the distribution for the highest flow rate (3 mL $min^{-1}$) shows a different amylose peak shifted to lower apparent sizes, which may be attributed to shear scission of amylopectin into amylose-sized moieties and/or poor separation at such fast flow rates. In the end, an optimal flow rate of 1.5 mL $min^{-1}$ was employed for the fractionation, since it offers the best resolution of the two populations present in starch with minimal apparent shear scission of the amylopectin component, and also has a similar linear velocity to that used for the same column set-up in analytical SEC separations.

Fractionations using preparative SEC were then implemented for amylose, glycogen, and native rice starch using the optimized experimental parameters of injected mass (1 mL × 20 g $L^{-1}$) and flow rate (1.5 mL $min^{-1}$). The size distributions obtained from the preparative-SEC fractionations are shown in Fig. 4 for amylose, glycogen, and rice starch. Eight fractions were collected from amylose and glycogen, and ten for rice starch. The fractionation conditions (elution volume ranges, $V_{el}$, and corresponding hydrodynamic radius, $\log(R_h/\mathrm{nm})_{PREP}$), for each sample are presented in Tables 1–3 for glycogen, amylose and rice starch, respectively.

### 3.2. Size distributions of the branched fractions from amylose, glycogen and starch

The different fractions from amylose, glycogen and starch obtained by preparative SEC were further analyzed using analytical SEC-MALLS-DRI in the 'branched' set-up to obtain the SEC weight distributions $w(\log V_h)$ and the size dependence of the weight-average molecular weight $\overline{M}_w(V_h)$, and are presented in Fig. 5. Size fractionation using preparative SEC was successful for all three polysaccharide samples, since the size distribution of the collected fractions fall under the envelope of the unfractionated (parent) sample in progressive order of fraction collection.

An average macromolecular size parameter for each fraction is defined [18] as the average hydrodynamic radius of the 'branched' distribution, $\log(\overline{R}_h)_{br}$, using an equivalent expression to the weight-average molecular weight for linear polymers (Eq. (2)).

$$\log(\bar{R}_h)_{br} = \frac{\int_{-\infty}^{\infty} w(\log\ V_h)\, d\ \log R_h}{\int_{-\infty}^{\infty}((w(\log V_h))/(\log R_h))\, d\ \log R_h} \quad (2)$$

Data for $\log(\overline{R}_h)_{br}$, together with the average-weight molecular weight from light-scattering calibration, $\overline{M}_w$, are presented for each 'branched' fraction in Tables 1–3 for glycogen, amylose, and rice starch, respectively.

Glycogen exhibits a relatively narrow monomodal size distribution for the unfractionated parent sample and for the respective fractions, with $\overline{M}_w$ values ranging between $2 \times 10^5$ and $1 \times 10^6$ g $mol^{-1}$ (Table 1 and Fig. 5a). The average macromolecular size $\log(\overline{R}_h)_{br}$ and molecular weight $\overline{M}_w$ show progressively smaller values with increasing fraction order, which demonstrates the suitability of the size fractionation using preparative SEC. A similar but slightly broader distribution is observed for the amylose sample, whose fractions display weight-average molecular weights in the range of $1 \times 10^5$–$2 \times 10^6$ g $mol^{-1}$ (Table 2 and Fig. 5b). The $\overline{M}_w$ distribution of the smallest fraction (A8) could not be experimentally obtained due to the low concentration and molecular weight of the macromolecular components of such fraction, which did not allow obtaining a suitable MALLS signal. Indeed, MALLS is especially suited for the analysis of macromolecules with high molecular weight but fails to provide accurate information for the smaller macromolecular populations which appear with lower concentrations in these samples. The size distributions of the collected fractions from native starch display the common profile for the two macromolecular populations present in starch, amylose and amylopectin, with average $\overline{M}_w$ values in the order of $10^8$–$10^9$ g $mol^{-1}$ for the amylopectin-rich fractions (S1–S6) and $10^5$–$10^6$ g $mol^{-1}$ for the amylose-rich fractions (S7–S10) (Table 3 and Fig. 5c). The size fractionation is successful, especially for the amylose-rich fractions, which are clearly apparent in the size distributions and the corre-

**Table 1**
Experimental parameters for the structural characterization of glycogen using multidimensional offline SEC.

| Sample | Preparative SEC fractionation | | Analytical SEC branched | | Analytical SEC debranched |
|---|---|---|---|---|---|
| | $V_{el}$ (mL) | Log $(R_h/nm)_{PREP}$ | Log $(\overline{R}_h/nm)_{br}$ | $\overline{M}_w$ (g mol$^{-1}$) | Log $(\overline{R}_h/nm)_{de}$ |
| Glycogen | – | – | 1.15 | $5.97 \times 10^5$ | 0.19 |
| G1 | 75–81 | 1.66–1.34 | 1.34 | $1.27 \times 10^6$ | 0.21 |
| G2 | 81–84 | 1.34–1.21 | 1.19 | $6.13 \times 10^5$ | 0.21 |
| G3 | 84–86.25 | 1.21–1.12 | 1.13 | $4.36 \times 10^5$ | 0.20 |
| G4 | 86.25–88.5 | 1.12–1.04 | 1.09 | $3.57 \times 10^5$ | 0.19 |
| G5 | 88.5–91.5 | 1.04–0.94 | 1.07 | $3.18 \times 10^5$ | 0.19 |
| G6 | 91.5–94.5 | 0.94–0.84 | 1.06 | $2.91 \times 10^5$ | 0.20 |
| G7 | 94.5–99 | 0.84–0.72 | 1.02 | $2.86 \times 10^5$ | 0.20 |
| G8 | 99–105 | 0.72–0.55 | 0.97 | $2.80 \times 10^5$ | 0.20 |

**Table 2**
Experimental parameters for the structural characterization of amylose using multidimensional offline SEC.

| Sample | Preparative SEC fractionation | | Analytical SEC branched | | Analytical SEC debranched |
|---|---|---|---|---|---|
| | $V_{el}$ (mL) | Log $(R_h/nm)_{PREP}$ | Log $(\overline{R}_h/nm)_{br}$ | $\overline{M}_w$ (g mol$^{-1}$) | Log $(\overline{R}_h/nm)_{de}$ |
| Amylose | – | – | 0.97 | $2.72 \times 10^5$ | 0.93 |
| A1 | 78.0–84.0 | 1.71–1.40 | 1.44 | $2.07 \times 10^6$ | 1.08 |
| A2 | 84.0–88.5 | 1.40–1.20 | 1.26 | $6.61 \times 10^5$ | 1.00 |
| A3 | 88.5–93.0 | 1.20–1.10 | 1.12 | $3.62 \times 10^5$ | 0.97 |
| A4 | 93.0–97.5 | 1.10–0.95 | 1.04 | $2.46 \times 10^5$ | 0.92 |
| A5 | 97.5–102.0 | 0.95–0.81 | 0.93 | $1.78 \times 10^5$ | 0.82 |
| A6 | 102.0–106.5 | 0.81–0.66 | 0.83 | $1.25 \times 10^5$ | 0.76 |
| A7 | 106.5–112.5 | 0.66–0.46 | 0.61 | $6.66 \times 10^4$ | 0.61 |
| A8 | 112.5–118.5 | 0.46–0.27 | 0.41 | – | 0.40 |

sponding averages. In the case of the amylopectin-rich fractions, some size separation is also observed despite the fact that large amylopectin populations lay beyond the exclusion limit of the pores and fractionation is thus limited (see Supplementary Data). Some deviations can be observed in the $\overline{M}_w(V_h)$ distributions for fractions S3 and S4, which are attributed to these technical limitations. In principle, field-flow fractionation (FFF) related technologies could overcome these SEC limitations, avoiding shear scission and effectively separating larger amylopectin molecules. Indeed, asymmetric-flow field-flow fractionation (AF$^4$) has been successfully applied to linear polysaccharides [33] and different branched polysaccharides of low to moderate molecular weight, including gum arabic [34], glycogen [35], and modified, degraded, and commercial starch-based polysaccharides [29,35–41]. However, obtaining reliable size distributions of fully dissolved undegraded native starch using FFF separation has been hindered by technical problems, such as aggregation, poor detection in solvents (particularly DMSO-based) which have been proven to fully dissolve starch without degradation, and calibration issues in the complex flows employed in the separation [18,42]. Present indications are that AF$^4$ cannot be used for size-separation characterization of native starch without major advances in technology. Moreover, obtaining sufficient sample for subsequent enzymatic debranching and size analyses with FFF-related technologies is limited by sample aggregation. Therefore, SEC still constitutes the most reliable procedure for obtaining size distributions for large polysaccharides, and its use in this study for the size fractionation and obtaining multidimensional size/branch distributions is fully justified.

### 3.3. Size distributions of the debranched fractions from amylose, glycogen and starch

The debranched SEC weight distributions $w(\log V_{h,de})$ for the collected fractions were obtained after enzymatic debranching with isoamylase and subsequent SEC analysis in the 'debranched' set-up. The $w(\log \overline{X}_{de})$ distributions can also be calculated by light-scattering measurements of the $\overline{M}_w$ of the debranched samples, which provide a weight-average degree of polymerization $\overline{X}_{de}$ at each slice of elution volume. Now, the $w(\log V_{h,de})$ and $w(\log \overline{X}_{de})$ distributions so obtained may not be the same, because of band-broadening effects and possible inaccuracy of the Mark–Houwink relation, for universal and light-scattering calibrations (used for $V_h$ and $\overline{X}_{de}$, respectively). The debranched distributions are presented in Fig. 6 for glycogen, amylose, and rice starch, showing distinct

**Table 3**
Experimental parameters for the structural characterization of native rice starch using multidimensional offline SEC.

| Sample | Preparative SEC fractionation | | Analytical SEC branched | | Analytical SEC debranched | | |
|---|---|---|---|---|---|---|---|
| | $V_{el}$ (mL) | Log $(R_h/nm)_{PREP}$ | Log $(\overline{R}_h/nm)_{br}$ | $\overline{M}_w$ (g mol$^{-1}$) | Zone AP1 Log $(\overline{R}_h/nm)_{de}$ | Zone AP2 Log $(\overline{R}_h/nm)_{de}$ | Zone AM3 Log $(\overline{R}_h/nm)_{de}$ |
| MRQ74 | – | – | 1.35 | $2.08 \times 10^8$ | 0.14 | 0.40 | 1.02 |
| S1 | 58.00–62.35 | 3.15–2.72 | 3.34 | – | 0.14 | 0.38 | – |
| S2 | 62.35–65.25 | 2.72–2.46 | 3.04 | $1.57 \times 10^9$ | 0.12 | 0.40 | – |
| S3 | 65.25–69.60 | 2.46–2.12 | 2.82 | $3.21 \times 10^8$ | 0.14 | 0.41 | – |
| S4 | 69.60–73.95 | 2.12–1.83 | 2.56 | $3.19 \times 10^8$ | 0.14 | 0.40 | – |
| S5 | 73.95–79.75 | 1.83–1.50 | 2.06 | $1.70 \times 10^8$ | 0.14 | 0.40 | 1.09 |
| S6 | 79.75–85.55 | 1.50–1.23 | 1.65 | $7.49 \times 10^7$ | 0.13 | 0.41 | 1.09 |
| S7 | 85.55–91.35 | 1.23–1.01 | 1.27 | $7.33 \times 10^6$ | 0.13 | 0.41 | 1.06 |
| S8 | 91.35–97.15 | 1.01–0.82 | 1.10 | $3.58 \times 10^6$ | 0.12 | 0.41 | 0.97 |
| S9 | 97.15–104.40 | 0.82–0.61 | 0.89 | $1.71 \times 10^6$ | 0.13 | 0.39 | 0.87 |
| S10 | 104.40–113.10 | 0.61–0.37 | 0.67 | $3.01 \times 10^5$ | 0.14 | 0.40 | 0.67 |

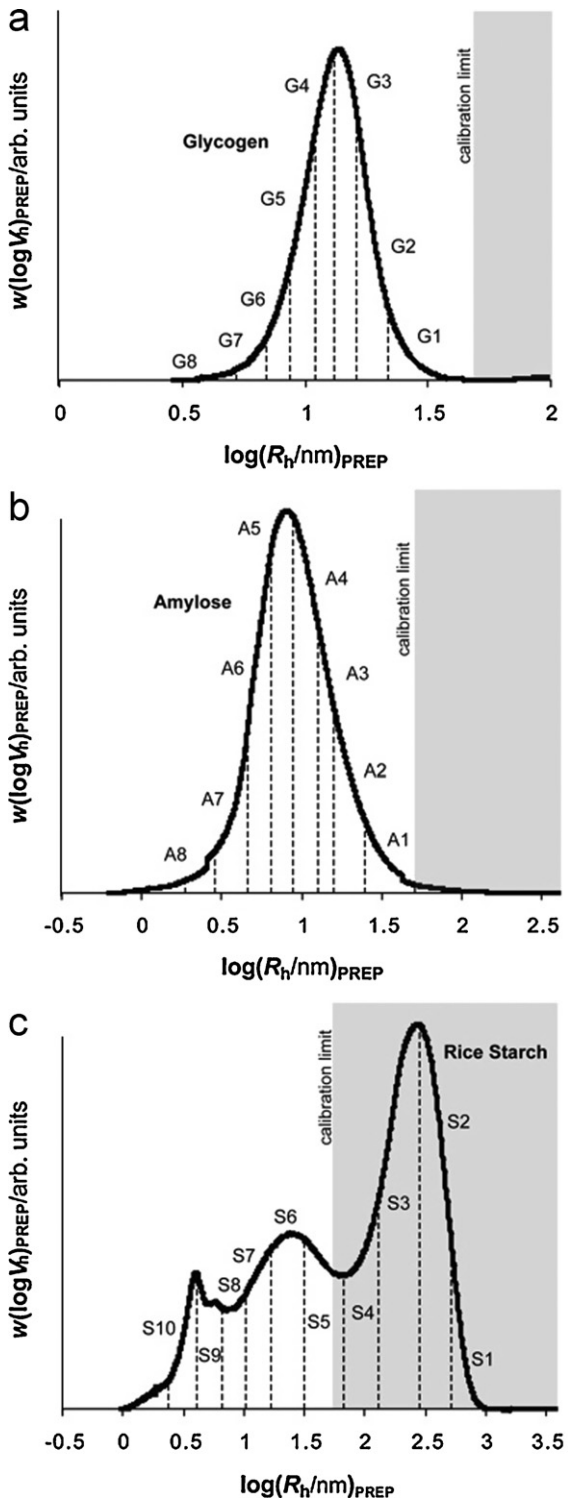


**Fig. 4.** Preparative SEC [$w(\log V_h)$] distributions indicating the collected fractions at different elution volumes (hydrodynamic radius): (a) glycogen; (b) amylose; (c) rice starch. The grey area corresponds to the extrapolated calibration region.

peaks corresponding to the short- and long-chain branches that in each case comprise the macromolecular architecture of the target branched polysaccharides. An average branch size $\log(\overline{R}_h)_{de}$ is defined for each branch population through Eq. (2).

Commercial glycogen debranched distributions show a monomodal peak with an average $\log(\overline{R}_h/\mathrm{nm})_{de} \sim 0.2$ ($\overline{X}_{de} \sim 15$), for both the whole and the collected fractions (Table 1). These monomodal distributions for the glycogen branches are consistent

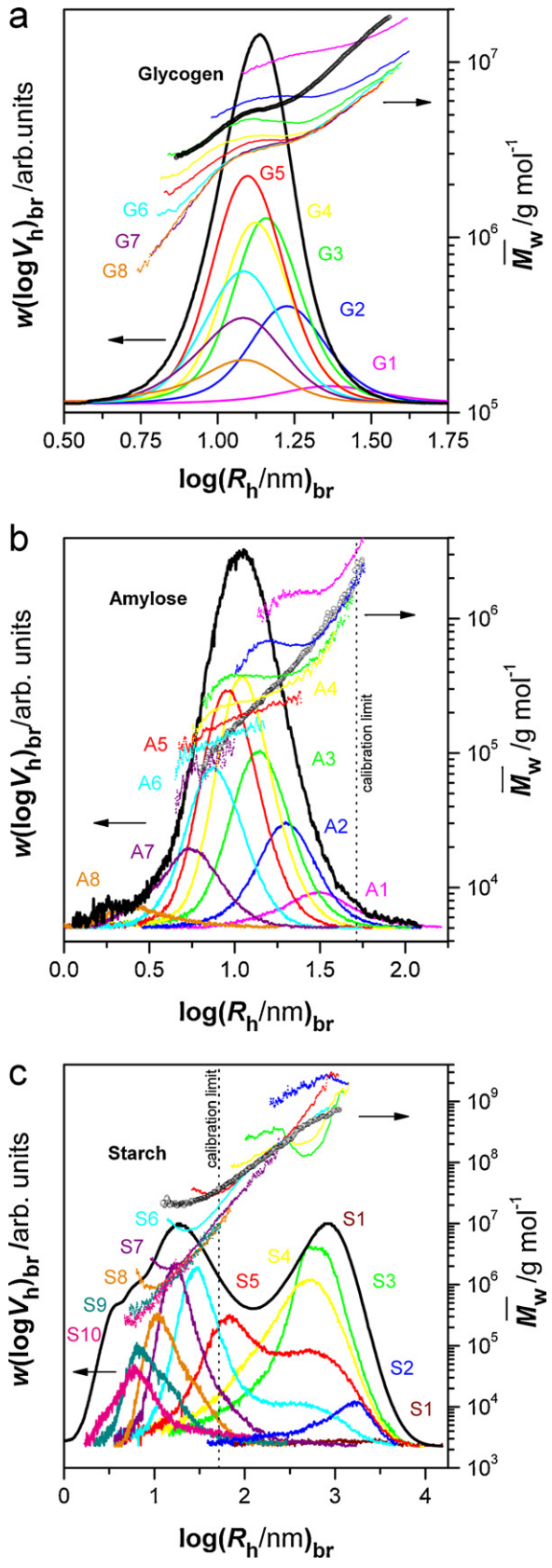


**Fig. 5.** SEC weight [$w(\log V_h)_{br}$] distributions for the branched collected fractions: (a) glycogen; (b) amylose; (c) rice starch. The different colours indicate the different size distributions for the collected branched fractions from preparative SEC. (For interpretation of the references to color in this figure legend, the reader is referred to the web version of the article.)

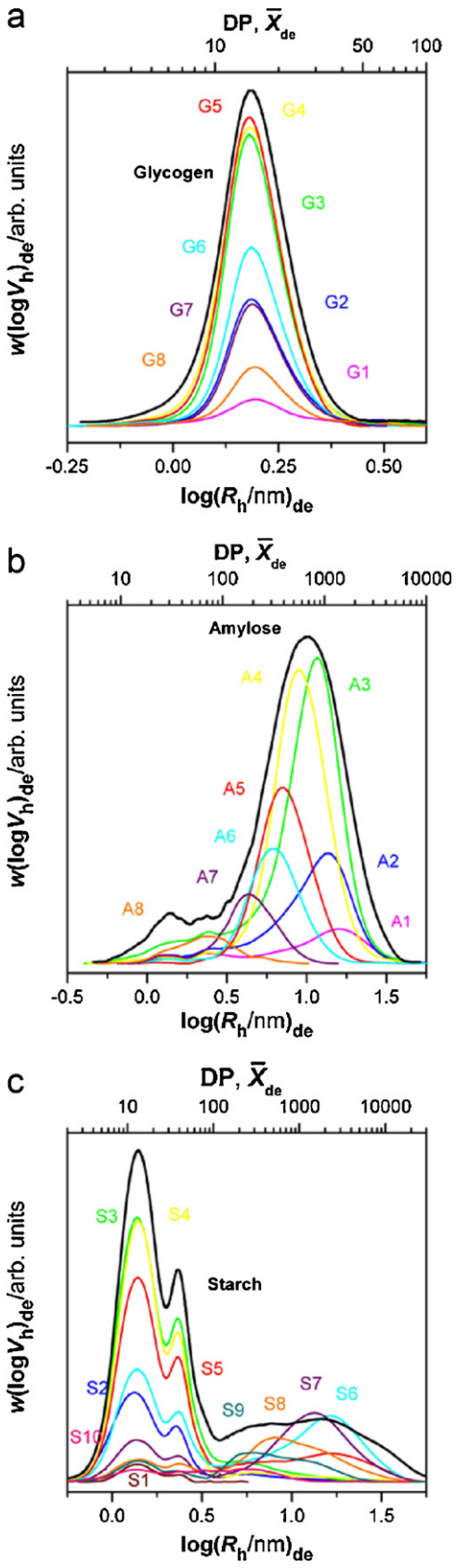


**Fig. 6.** SEC weight [$w(\log V_h)_{de}$] distributions for the debranched collected fractions: (a) glycogen; (b) amylose; (c) rice starch. The different colours indicate the different size distributions for the collected debranched fractions from preparative SEC. (For interpretation of the references to color in this figure legend, the reader is referred to the web version of the article.)

with the chain-length distributions given by other authors for glycogen from oyster [43] and various mammals [2].

Commercial amylose exhibits debranched size distributions that are progressively shifted to lower sizes with increasing fraction order. As expected, because amylose is long-chain branched, the average size of the branches is larger for amylose than for the short-chain-branched glycogen and amylopectin: for amylose, the average branch length ranges between $\log(\overline{R}_h)_{de}/nm \sim 0.4 - 1.0$ ($\overline{X}_{de} \sim 100–4000$) for the different fractions (Table 2). Some amylose fractions also show small peaks at smaller sizes, which may correspond to smaller amylopectin branch impurities from the industrial separation procedure, although multi-modal chain-length distributions are found in amylose from native starch (e.g. [44]).

The distributions for starch (Table 3) are similar to those reported and discussed previously [18]. The amylopectin debranched distributions are independent of total starch-molecule size, whereas the debranched distributions for the amylose populations in native starch show decreasing size with decreasing macromolecular size; the latter behaviour is also seen here for commercial amylose.

### 3.4. 2D structural size/branching distributions for branched polysaccharides

The 2D distributions $w[\log(\overline{R}_h)_{br}, \log X_{de}]$ were constructed as follows. A 3-dimensional array was first calculated with the experimental results, using $\log(\overline{R}_h)_{br}$ as variable $X$, $\log \overline{X}_{de}$ as variable $Y$, and $w(\log X_{de})$ as variable Z. Renka–Cline random gridding mathematical procedure was applied using Origin 7.0 Software (OriginLab Corporation, MA, USA) to construct an interpolating surface to the scattered experimental data from the 3-variable matrix. The surface so constructed, which is continuous and has continuous first derivatives, is the desired 2D structural size/branching distribution $w[\log(\overline{R}_h)_{br}, X_{de}]$. Similarly, the equivalent 2D distribution $w(\log(\overline{M}_w)_{br}, \log X_{de})$ was constructed using the weight-average molecular weight $\overline{M}_w(V_h)$ of the branched polymers as the first dimension and the corresponding branch-size distributions $w(\log X_{de})$ of the debranched fractions as the second dimension. While these distributions are simple transformations of each other, because the first axes in each case are related by the measured quantity $\overline{M}_w(V_h)$ of the branched polymers, it is useful to present the data in these two equivalent ways, as it is common to think of distributions in terms of molecular weight rather than in terms of size. However, it must be emphasized that this molecular weight is a (weight) *average*, because for complex branched polymers there is no one-to-one correspondence between size and molecular weight. It is also noted that the two forms of the $X$-axis, $\overline{M}_w$ from MALLS and $R_h$ from universal calibration, will not be exactly equivalent because of artifacts from band broadening and any inaccuracy of universal calibration.

Figs. 7 and 8, respectively, show the 2-dimensional $w[\log(\overline{R}_h)_{br}, \log X_{de}]$ and $w[\log \overline{M}_w, \log X_{de}]$ distributions for commercial glycogen, commercial amylose, and native rice starch. These 2-dimensional branch/size distributions have potential to elucidate (bio)synthesis–structure–property relations, for example using theory developed for these purposes [10,45]. To facilitate discussion, the structures at the individual branch and at the full macromolecular size level for glycogen, amylose, and native starch macromolecular populations are sketched in Fig. 9.

The 2-dimensional size/branch distribution of commercial glycogen shows a single topological feature corresponding to medium macromolecular sizes and small branch sizes. The surface is monomodal and symmetrical, the axis of symmetry being the average chain length of the debranched size distributions at $\overline{X}_{de} \sim 15$. The monomodal and symmetrical nature of the surface

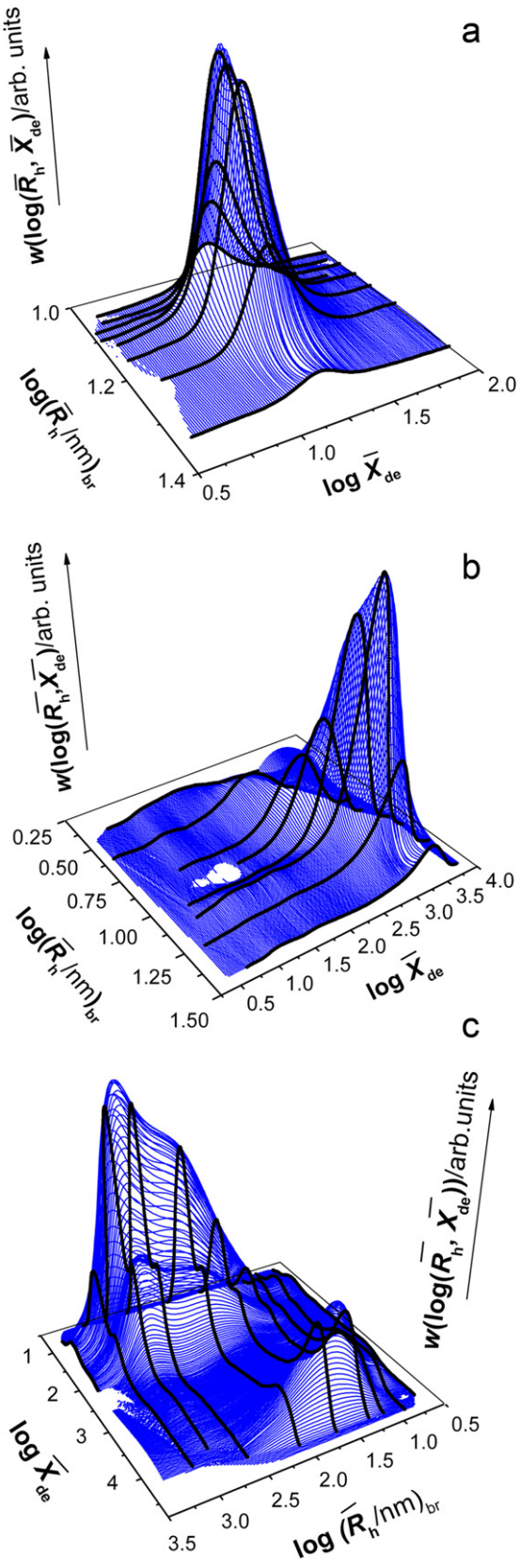


**Fig. 7.** 2-Dimensional SEC weight distribution $w[\log(\overline{R}_h)_{br}, X_{de}]$ based on macromolecular and branch size: (a) glycogen; (b) amylose; (c) rice starch. The black points correspond to the experimental data from each collected fraction from preparative SEC. The blue surfaces are the distributions obtained after Renka–Cline random gridding. (For interpretation of the references to color in this figure legend, the reader is referred to the web version of the article.)

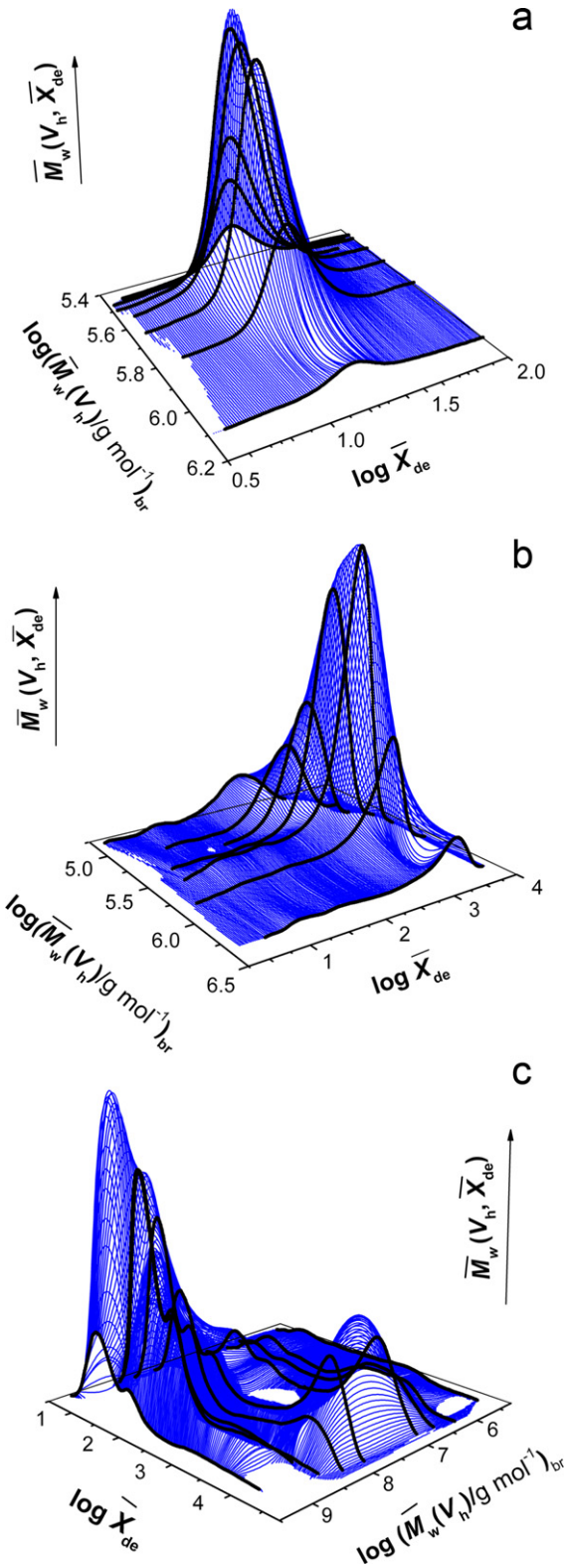


**Fig. 8.** 2-Dimensional $w(\log(\overline{M}_w), \log X_{de})$ distributions: (a) glycogen; (b) amylose; (c) rice starch. The black points correspond to the experimental data from each collected fraction from preparative SEC. The blue surfaces are the distributions obtained from Renka–Cline random gridding. (For interpretation of the references to color in this figure legend, the reader is referred to the web version of the article.)

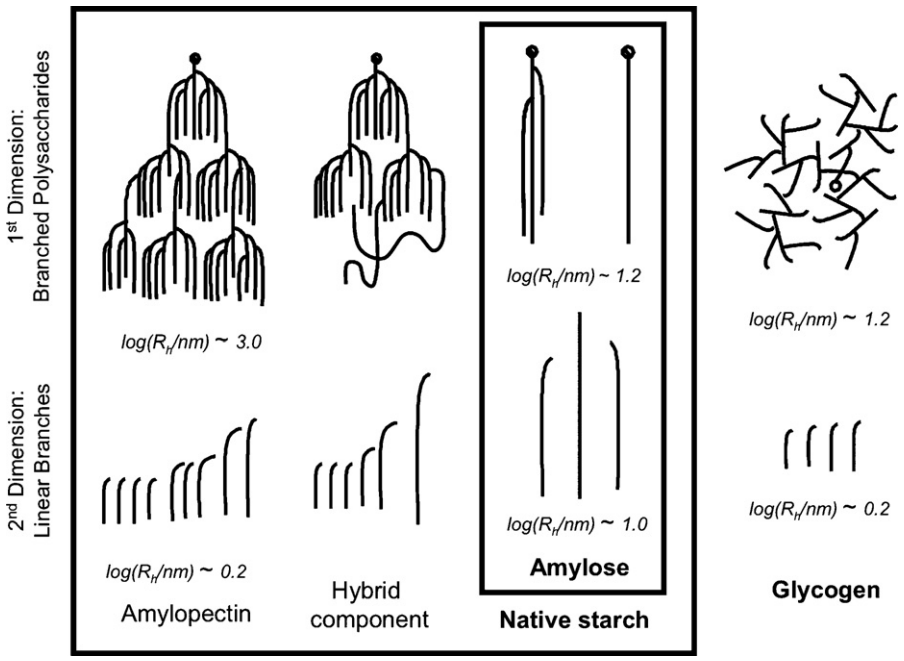


**Fig. 9.** Sketches of the individual branch and macromolecular structures of the branched polysaccharides considered in this study. $R_h$ values are nm in each case.

shows a homogeneous branching structure for all macromolecular sizes, with a single distribution of branch lengths irrespective of macromolecular size. This independence of the branching structure on overall macromolecular size implies that the activities of the enzymes controlling the branch-length distribution (glycogen synthase and branching enzymes) are unaffected by the size of the whole molecule. This can be rationalized by the assumption that during biosynthesis, the glycogen molecules are of relatively low 'molecular density', or 'dispersed molecular density' [46], of the isolated molecule in solution, defined by:

$$\rho(V_h) = \frac{\overline{M}_w(V_h)}{(\overline{R}_g(V_h))^3} \quad (3)$$

This gives the relative amount of 'solid' polysaccharide in the solvent-swollen isolated molecule. The approximate average $\rho$ values for the amylose, rice starch, and glycogen parent samples are 40.8, 9.8, and 84.9 g mol$^{-1}$ nm$^{-3}$, which are consistent with those reported by Jane et al. in an aqueous system [46]. These are for the macromolecule in the solvent system employed for separation and may differ from those for their biosynthesis.

The 2-dimensional distribution for commercial amylose also displays a single topological surface but with a multimodal shape in both macromolecular sizes and chain lengths, evidencing a variable branching architecture for this macromolecule. These multimodal branch size components may correspond to the linear and the long-chain branched populations of amylose, and/or different starch-synthase enzymes in different loci (e.g. granule-bound starch synthase and soluble starch synthases [47]). The branch sizes are of the same order of magnitude as the original macromolecules, as is expected for a chain branched macromolecule with a small (but significant) amount of long-chain branching. However, for the case of amylose, there is (unlike glycogen) an evident relation between the size of the branches and macromolecular size, which is also seen for the amylose component of native starch in the same figures and reported earlier [18] (and therefore suggesting that this is not an artifact of any degradation that the commercial amylose would have undergone during preparation of the commercial sample). This indicates that macromolecular size influences the enzymatic reactions for this component during starch granule generation, as discussed previously [18]. Quantification of this observation, such as fitting to functional forms suggested by models (e.g. [45]) must await corrections for band broadening, which can induce significant changes in the quantitative shape of the distribution [48].

The 2D distributions for native starch are similar to those reported and discussed previously [18].

## 4. Conclusions

A systematic analytical methodology has been developed, optimized and applied to different branched glucose polysaccharides (commercial glycogen, commercial amylose, and native starch) to obtain 2-dimensional structural distributions based on macromolecular size and branch length. The 2D distributions of these polysaccharides display characteristic topological surfaces. Commercial glycogen exhibits a single monomodal symmetrical surface, which corresponds with a single population of branches that arrange themselves to create a homogeneous branching structure independently of macromolecular size; this suggests that the molecular density ('space' between branches) of glycogen during biosynthesis is sufficiently low that enzyme activity is relatively unimpeded by surrounding branches. Amylose (both commercial and as a component in native starch), on the other hand, displays a single topological feature, but which is multimodal and scattered throughout macromolecular sizes, indicating a heterogeneous branching architecture, probably arising from different biosynthesis loci in the growing grain. The 2D distributions for native starch show distinct and separated topological features, corresponding to amylopectin, amylose, and hybrid populations that differ in macromolecular size and branch chain length.

Two-dimensional size/branch distributions have considerable potential for the topological differentiation of glycogen and starch samples from different tissues, species and plant varieties, respectively, providing additional and hitherto hidden information about the fine branching features of such macromolecules. For example, glycogen is the glucose buffer in human body, which is biosynthesised and degraded repeatedly according to the energy needs of the organism. The methodology may shed light on diabetes, because glucose concentrations, which are poorly controlled in this disease,

are regulated by glycogen biosynthesis and biodegradation. The methodology could have immediate applicability in the structural elucidation of so-called 'high-amylose' starches, which are starch mutants with longer chain lengths with nutritional benefits (e.g. [49]).

## Acknowledgments

FV greatly appreciates the support of a postdoctoral fellowship from the Knut and Alice Wallenberg Foundation (Sweden), and we gratefully acknowledge the support of the Australian Research Council (DP0985694 and DP0986043). Dr. Richard A. Cave is thanked for his support in setting up the preparative SEC fractionation. Dr. Kinnari Shelat is thanked for performing the reduced viscosity measurements.

## Appendix A. Supplementary data

Supplementary data associated with this article can be found, in the online version, at doi:10.1016/j.chroma.2011.05.027.

## References

[1] P.C. Calder, Int. J. Biochem. 23 (1991) 1335.
[2] J.-H. Ryu, J. Drain, J.H. Kim, S. McGee, A. Gray-Weale, L. Waddington, G.J. Parker, M. Hargreaves, S.-H. Yoo, D. Stapleton, Int. J. Biol. Macromol. 45 (2009) 478.
[3] C.E. Ioan, T. Aberle, W. Burchard, Macromolecules 32 (1999) 7444.
[4] A. Buleon, P. Colonna, V. Planchot, S. Ball, Int. J. Biol. Macromol. 23 (1998) 85.
[5] R.G. Jones, J. Kahovec, R. Stepto, E.S. Wilks, M. Hess, T. Kitayama, W.V. Metanomski, Compendium of Polymer Terminology and Nomenclature, IUPAC Recommendations 2008, Royal Society of Chemistry, Cambridge, 2009.
[6] A.E. Hamielec, A.C. Ouano, J. Liq. Chromatogr. 1 (1978) 111.
[7] A.E. Hamielec, A.C. Ouano, L.L. Nebenzahl, J. Liq. Chromatogr. 1 (1978) 527.
[8] L.K. Kostanski, D.M. Keller, A.E. Hamielec, J. Biochem. Biophys. Methods 58 (2004) 159.
[9] F. Vilaplana, R.G. Gilbert, J. Sep. Sci. 33 (2010) 3537.
[10] A. Gray-Weale, R.G. Gilbert, J. Polym. Sci. Part A: Polym. Chem. Ed. 47 (2009) 3914.
[11] D.M. Meunier, P.B. Smith, S.A. Baker, Macromolecules 38 (2005) 5313.
[12] R. Edam, D.M. Meunier, E.P.C. Mes, F.A. Van Damme, P.J. Schoenmakers, J. Chromatogr. A 1201 (2008) 208.
[13] T. Chang, H.C. Lee, W. Lee, S. Park, C. Ko, Macromol. Chem. Phys. 200 (1999) 2188.
[14] J. Adrian, E. Esser, G. Hellmann, H. Pasch, Polymer 41 (2000) 2439.
[15] A. van der Horst, P.J. Schoenmakers, J. Chromatogr. A 1000 (2003) 693.
[16] P. Kilz, R.P. Kruger, H. Much, G. Schulz, Adv. Chem. Ser. 247 (1995) 223.
[17] P. Kilz, Chromatographia 59 (2004) 3.
[18] F. Vilaplana, R.G. Gilbert, Macromolecules 43 (2010) 7321.
[19] N. Libessart, M.L. Maddelein, N. Vandenkoornhuyse, A. Decq, B. Delrue, G. Mouille, C. Dhulst, S. Ball, Plant Cell 7 (1995) 1117.
[20] A. Tziotis, K. Seetharaman, K.S. Wong, J.D. Klucinec, J.L. Jane, P.J. White, Cereal Chem. 81 (2004) 611.
[21] J. Rosselgong, S.P. Armes, W.R.S. Barton, D. Price, Macromolecules 43 (2010) 2145.
[22] R.G. Gilbert, M. Hess, A.D. Jenkins, R.G. Jones, P. Kratochvil, R.F.T. Stepto, Pure Appl. Chem. 81 (2009) 351.
[23] M.K. Morell, M.S. Samuel, M.G. O'Shea, Electrophoresis 19 (1998) 2603.
[24] M.G. O'Shea, M.S. Samuel, C.M. Konik, M.K. Morell, Carbohydr. Res. 307 (1998) 1.
[25] R.A. Cave, S.A. Seabrook, M.J. Gidley, R.G. Gilbert, Biomacromolecules 10 (2009) 2245.
[26] N.-L. Hoang, A. Landolfi, A. Kravchuk, E. Girard, J. Peate, J.M. Hernandez, M. Gaborieau, O. Kravchuk, R.G. Gilbert, Y. Guillaneuf, P. Castignolles, J. Chromatogr. A 1205 (2008) 60.
[27] S. Schmitz, A.C. Dona, P. Castignolles, R.G. Gilbert, M. Gaborieau, Macromol. Biosci. 9 (2009) 506.
[28] Z.A. Syahariza, E. Li, J. Hasjim, Carbohydr. Polym. 82 (2010) 14.
[29] C.C. Rojas, K.-G. Wahlund, B. Bergenstahl, L. Nilsson, Biomacromolecules 9 (2008) 1684.
[30] A.M. Striegel, W.W. Yau, J.J. Kirkland, D.D. Bly, Modern Size-exclusion Liquid Chromatography – Practice of Gel Permeation and Gel Filtration Chromatography, John Wiley & Sons, Hoboken, NJ, 2009.
[31] A.M. Striegel, J. Liq. Chromatogr. Relat. Technol. 31 (2008) 3105.
[32] H.G. Barth, F.J. Carlin, J. Liq. Chromatogr. 7 (1984) 1717.
[33] B. Wittgren, K.-G. Wahlund, J. Chromatogr. A 760 (1997) 205.
[34] L. Picton, I. Bataille, G. Muller, Carbohydr. Polym. 42 (2000) 23.
[35] A. Rolland-Sabate, P. Colonna, M.G. Mendez-Montealvo, V. Planchot, Biomacromolecules 8 (2007) 2520.
[36] M. van Bruijnsvoort, K.G. Wahlund, G. Nilsson, W.T. Kok, J. Chromatogr. A 925 (2001) 171.
[37] P. Roger, B. Baud, P. Colonna, J. Chromatogr. A 917 (2001) 179.
[38] S. Lee, P.O. Nilsson, G.S. Nilsson, K.G. Wahlund, J. Chromatogr. A 1011 (2003) 111.
[39] S. Lee, S.T. Kim, B.R. Pant, H.D. Kwen, H.H. Song, S.K. Lee, S.V. Nehete, J. Chromatogr. A 1217 (2010) 4623.
[40] S. You, S.G. Stevenson, M.S. Izydorczyk, K.R. Preston, Cereal Chem. 79 (2002) 624.
[41] K.-G. Wahlund, M. Leeman, S. Santacruz, Anal. Bioanal. Chem. 399 (2011) 1455.
[42] R.G. Gilbert, Anal. Bioanal. Chem. 399 (2011) 1425.
[43] M. Matsui, M. Kakut, A. Misaki, Carbohydr. Polym. 31 (1996) 227.
[44] R.M. Ward, Q. Gao, H. de Bruyn, R.G. Gilbert, M.A. Fitzgerald, Biomacromolecules 7 (2006) 866.
[45] A.C. Wu, R.G. Gilbert, Biomacromolecules 11 (2010) 3539.
[46] S.-H. Yoo, J. Jane, Carbohydr. Polym. 49 (2002) 307.
[47] S.G. Ball, M.K. Morell, Ann. Rev. Plant Biol. 54 (2003) 207.
[48] K.Y. van Berkel, G.T. Russell, R.G. Gilbert, Macromolecules 38 (2005) 3214.
[49] J.D. Klucinec, D.B. Thompson, Cereal Chem. 75 (1998) 887.